# Machine Learning Based Blockage Prediction in Mm-wave V2I Communications

1st Yuya Sugimoto

Electrical and Electronic Engineering

Institute of Science Tokyo

Tokyo, Japan

sugimoto.y.ag@m.titech.ac.jp

2<sup>nd</sup> Gia Khanh Tran
Electrical and Electronic Engineering
Institute of Science Tokyo
Tokyo, Japan
ORCID: 0000-0001-5190-1085

Abstract—This paper shows how to predict mm-Wave enabled V2I (Vehicle to Infrastructure) communication quality. These days, automated driving is widespread. However, there are blind spots that cannot be recognized by the sensors installed on the vehicles. To circumvent this, infrastructure i.e. RSU (Road Side Unit) which is equipped with camera, LiDAR, which is a sensor that can emit laser beams and uses the information from the reflected light to measure the distance to an object and the shape of the object on the vehicles and antenna can send information to the vehicles. This paper attempts to predict such V2I communication quality merely based on images from the RSU camera. We propose a comprehensive prediction method that focuses on V2I scenarios and Numerical analyses were conducted to predict changes in received power of mm-Wave enabled V2I communication links in a complete simulation environment.

Index Terms—V2I, Deep Learning, mm-Wave, Prediction

#### I. Introduction

Automated driving is becoming increasingly widespread, paving the way for the realization of Cooperative Perspective Systems (CPS). CPS also means Cyber Physical System. The system uses the advanced computational capabilities of cyber systems to compute physical systems with many uncertainties and feed them back to the real world [1]. CPS enables vehicles to communicate with other vehicles (V2V) and roadside units (RSUs) (V2I), allowing them to perceive dynamic road and intersection environments collaboratively. Through this communication, vehicles can receive critical information about pedestrians, bicycles, and other vehicles, even in blind spots, by relying on data shared by other vehicles or RSUs. Our focus is on V2I communication in large intersections. For smaller intersections, the 5.9 GHz wavebands are expected to be sufficient. However, large intersections often involve a high density of vehicles, which can strain the available bandwidth. To address this, we consider the use of mmWave bands due to their wide bandwidth and high-capacity communication capabilities [2]. While mmWave bands offer significant advantages over 5.9 GHz, they are more susceptible to blockage losses. To effectively apply mmWave communication in large intersections, particularly for scenarios involving a large number of vehicles, high-speed moving objects, and environments obstructed by large vehicles, more advanced beamforming technologies will be essential. These technologies will be critical for ensuring

reliable communication and overcoming the challenges posed by such complex environments. Vehicle-to-everything system together with AI can acquire the information from various sources, can expand the driver's perception, and can predict to avoid potential accidents, thus enhancing the comfort, safety, and efficiency [3].

In dynamic environments, V2I communication must remain uninterrupted, as vehicles, pedestrians, and bicycles are constantly in motion. To address this, we focus on predicting V2I communication quality using cameras installed on RSUs. There are also several previous researches on estimating propagation loss without using images. To predict propagation loss, machine learning is one of effective methods and various information are used for input data. Reccurent Neural Network (RNN) can analyze time series data of received power, and can be applied for 2- 26GHz communications [4]. When not only received power, but also environmental data such as distance and whether LOS (Line Of Site) or not is used for machine learning, prediction accuracy has improved [5]. Convolutional Neural Networks (CNN) is also used for prediction because it can recognize images. Images of building map and environmental information for machine learning show some degree of prediction accuracy [6]. However, this map images are taken from sky, so it is difficult for applying to dynamic situation.

Previous research has explored mmWave blockage prediction in small-scale areas [7]. This study utilizes stereo camera images combined with CNN for prediction. However, the experimental setup in this prior work assumes an open environment, such as a large parking lot, devoid of obstacles. In contrast, the practical application of this prediction technology is in urban intersections, where numerous buildings create complex environments. As a result, propagation paths involving reflections must also be considered to accurately predict V2I communication quality in such scenarios.

Another prior study explores blockage prediction using stereo vision through CARLA, an open-source urban driving simulator [8]. In this research, driving simulator images are utilized to predict signal obstruction. However, as CARLA is not a dedicated communication simulation platform, it cannot calculate specific received power values. Instead, it only determines whether a signal is obstructed or not. In real-world scenarios, the degree of obstruction depends on factors such as

the size and number of vehicles, making a binary distinction between "shielded" and "non-shielded" insufficient for practical applications. The machine learning methods employed in this study include 3D convolutional layers, LSTM layers, and standard convolutional layers. Additionally, another study focuses on real-time throughput measurement using depth images in millimeter-wave communications [9]. This research specifically addresses shielding caused by a person crossing the signal path. The machine learning algorithm applied is an extension of AROW (Adaptive Regularization of Weight Vectors) tailored for regression tasks. While these approaches offer insights, they are limited in scope and do not fully capture the complexity of urban communication scenarios with diverse and dynamic obstructions.

In this paper, in contrast to conventional method, mm-wave blockage prediction is applied and evaluated in a virtual digital twin. Specifically, we utilize Wireless InSite [10] for graphical simulations of radio wave propagation using the ray-tracing method. This method, based on geometric optics approximation, models the propagation paths of radio waves as if they were light rays. Building on this, we propose a comprehensive prediction method tailored for V2X communication, capable of predicting received power within a fully simulated environment. This approach provides detailed insights into signal behavior, enabling more precise and reliable communication performance evaluations.

# II. SIMULATION ENVIRONMENT

# A. Simulation Setup

A schematic diagram of the simulation environment is shown in Fig. 1. Simulation parameter is shown in Table I.

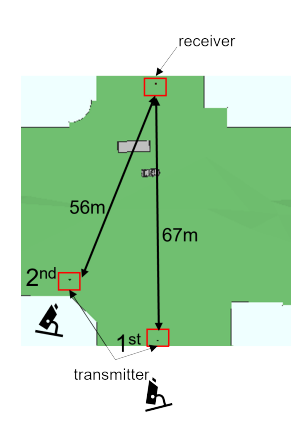


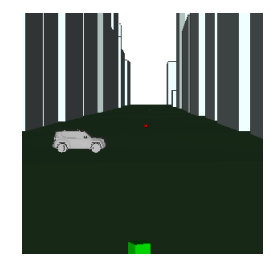
Fig. 1: simulation environment

In our simulation setup, we assumed two RSUs: one positioned directly in front of the vehicle (1st RSU) and the other diagonally in front (2nd RSU). Transmitters and receivers were placed either 67 m or 57 m apart, facing each other. The received power was measured as the vehicle moved at 0.5 m intervals. Assuming the vehicle entered the intersection at a speed of 5 m/s (18 km/h), with 10 images captured per second, the movement corresponded to 0.5 m increments per frame. The images were taken such that the transmitter was

TABLE I: Simulation parameters

Parameter	Transmitter	Receiver
Frequency	60GHz	60GHz
Bandwidth	2.5GHz	2.5GHz
Power	20dBm	
Noise Figure		3dB
Antenna	Half-wave dipole	Half-wave dipole
Height	2m	1.4m
Reflections	4	
Transmissions	0	
Diffractions	1	

positioned at the bottom center of the frame and the receiver at the middle center. For the simulation environment, large intersections near Tokyo Station were imported from Plateau [11], a website that provides open data on 3D urban models. Camera angles from the perspectives of the 1st and 2nd RSUs are illustrated in Figs. 2a and Figure 2b respectively.





(a) 1st camera angle.

(b) 2nd camera angle.

Fig. 2: Camera angle.

The simulation includes four 3D vehicle models: car, jeep, truck, and bus. Various scenarios were considered to evaluate performance. First, each vehicle moves independently from left to right. Second, a car and a jeep run either side-by-side or in opposite lanes, simulating interactions between vehicles of similar size. Finally, a bus and a car run either side-by-side or in opposite lanes, representing interactions between vehicles of different sizes. The experiments involving two vehicles were repeated five times, each with varying vehicle spacing. As a result, the simulation includes a total of 24 scenarios. Each dataset consists of 37 images with corresponding labels, resulting in a total of 888 data points.

# B. Machine Learning

CNN (Convolutional Neural Network) is a kind of machine learning methods and has been used widely in the field of Image Recognition. It has two characteristic layers.

The first layer, known as the Convolutional Layer, operates by applying small regions called filters to the image. These filters slide across the image, processing one region at a time and compressing each region into a single feature value. This layer enables feature extraction based on regions of the image rather than individual points, providing a more comprehensive representation of spatial features.

The second layer, known as the Pooling Layer, uses a technique called Max Pooling. In this process, a small region (filter) is applied to the image, and the highest numerical value

within the region is selected as the feature value. This layer also plays a crucial role in reducing the spatial resolution of the feature map, simplifying the representation while preserving important features.

Finally, the output from the previous layer is passed through fully connected layers to generate the final predictions.

To create the machine learning dataset, input images are resized to  $300 \times 300$  pixels, and the label data corresponds to the received power at the receiver. The received power values are normalized to facilitate efficient learning. For testing, data from one scenario of each two-vehicle experiment is excluded, resulting in four distinct scenarios used as test data. Consequently, the dataset is divided into 148 test samples and 740 training samples. Machine learning models is constructed based on previous studies [7].

Machine learning can be categorized into different types based on how the data is processed during training. In batch learning, the entire training dataset is processed at once. In contrast, mini-batch learning divides the dataset into smaller, pre-determined batches that are trained sequentially. Online learning takes a different approach, training the model incrementally by processing data one sample at a time and updating the estimation results continuously. For dynamic environments like intersections, online learning is particularly advantageous, as it allows for real-time updates to the learning results, adapting quickly to changing conditions.

TABLE II: Machine learning parameters

#### (a) PARAMETER

#### (b) LAYER SEQUENCE

parameter	value
training data	740
test data	148
epoch	100
batch size	1
optimizer	SGD
learning rate	0.001
loss function	MSE

Layer
Convolutional 1
Max Pooling 1
Convolutional 2
Max Pooling 2
Flatten
Fully Connected
output

## III. NUMERICAL ANALYSIS RESULTS

In this section, we present the results obtained under the conditions described in the previous chapter. The next figures illustrate these outcomes. First, we analyze the results from the 1st RSU, focusing on the impact of communication attenuation caused by vehicles and examining the error between simulated and predicted values. After that, we evaluate the combined results from the 1st and 2nd RSUs, demonstrating the effectiveness of using predictions to optimize the selection of multiple RSUs.

# A. Scenario of using a single RSU

The results of the car and jeep running side-by-side are shown in Fig. 3. As illustrated in the image, there is a gap between the two vehicles, allowing for a momentary Line of Sight (LOS). The figure demonstrates that higher received power can be predicted only when the receiver is positioned between the two vehicles. Since the car and jeep are similar

in size, the propagation loss is believed to remain relatively consistent.

The results of the car and jeep running in opposite lanes are shown in Fig. 4. The original data indicate that received power is particularly low when the two vehicles overlap. However, since the vehicles are moving in opposite lanes, the duration of low received power is shorter compared to when they run side-by-side. Additionally, even during overlap, some received power may be obtained through reflections, making it challenging to accurately predict subtle increases or decreases in received power.

The results of the bus and car running side-by-side are shown in Fig. 5. As depicted in the image, the car is slightly ahead of the bus. Naturally, the large body of the bus has a greater shielding effect, resulting in lower received power later in the scenario compared to the beginning. When only the car is between the transmitter and receiver, the received power prediction tends to be unstable. In contrast, the prediction becomes more stable and accurate when the bus is in the communication path. This stability is attributed to the bus's large body, which is easily recognized as an obstruction. However, there is still room for improvement in the accuracy of received power predictions.

The results of the bus and car running in opposite lanes are shown in Fig. 6. Due to the large size of the bus, the shielding effect of the car is minimal, even when the car and bus pass directly in front of the receiver. The significant fluctuations in the original data at the beginning may be attributed to reflections, diffraction, or possibly a simulation artifact. Nevertheless, the predictions effectively capture the points where the received power begins to decrease and when it returns to normal levels.

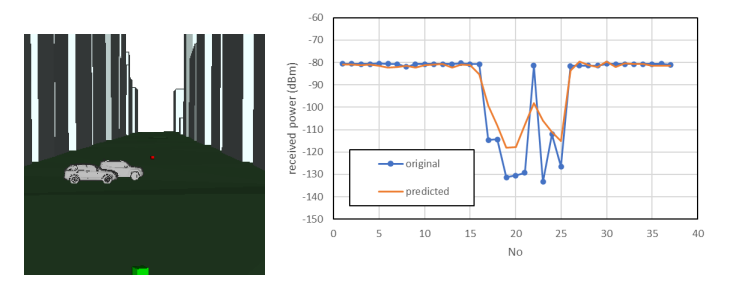


Fig. 3: Car and jeep running side-by-side (1st RSU).

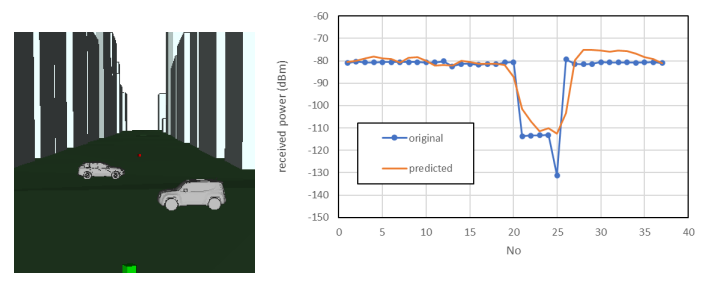


Fig. 4: Car and jeep running in opposite lane (1st RSU).

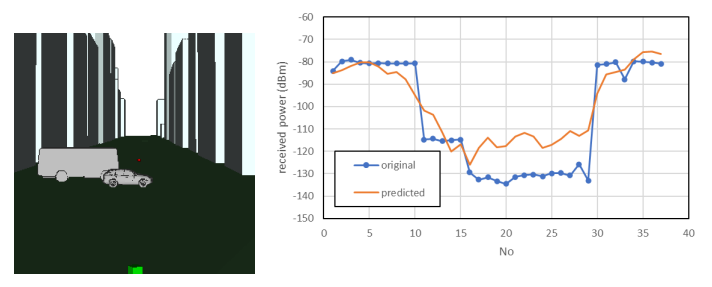


Fig. 5: Bus and car running side-by-side (1st RSU).

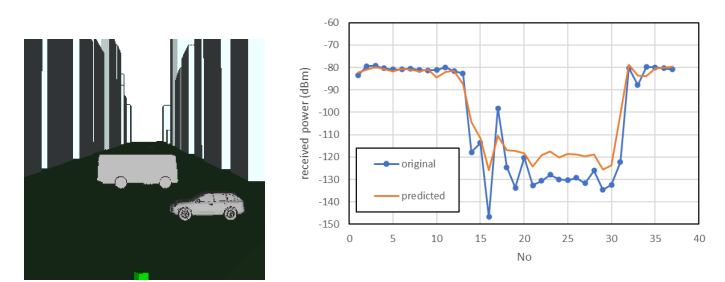


Fig. 6: Bus and car running in opposite lane (1st RSU).

# B. Scenarios of selection among different RSUs

This section presents the simulated and predicted values for both RSUs simultaneously and the numerical results are shown in Figs. 7- 14. To optimize communication, the RSU with the higher received power should be utilized, as indicated by the colored indicators above the figure i.e. orange for the 1st RSU and yellow for the 2nd RSU. As shown in the figure, the 2nd RSU generally has higher received power without blockage, which is expected since it is closer to the receiver, as presented in Section II-A. Notably, the RSU selection can be effectively determined based on predicted received power. If RSUs are chosen using the predicted values and the simulated values align with the actual received power, whether large or small, the system can be considered highly accurate and reliable.

For example, the results of the car and jeep running side-byside are shown in Fig. 8. By examining the predicted values for the 1st RSU (orange) and the 2nd RSU (yellow) in the figure, the color-coded bar above indicates which RSU is selected based on the higher predicted value. In this case, the agreement between the simulated and predicted received power values confirms that the RSUs were accurately selected to optimize communication efficiency.

It is important to understand the reasoning behind this RSU selection. In this scenario, both vehicles are moving from left to right, initially positioning the 2nd RSU and the receiver in a Line of Sight (LOS) configuration. As the vehicles progress, the diagonal left angle from the 2nd RSU becomes obstructed. In this zone, the 1st RSU is utilized. When the vehicles reach the center of the intersection and enter a blind spot from the 1st RSU, the 2nd RSU is then selected to maintain communication from the opposite direction. After position No. 26, there are no obstructions from either RSU, resulting in

an LOS environment. However, the 2nd RSU continues to be selected due to its closer proximity to the receiver.

The results of the car and jeep running in opposite lanes are shown in Fig. 10. The selection of RSUs during signal obstruction follows the same approach as described in Fig. 8. However, between positions No. 28 and No. 33 (highlighted in red), the predicted values for the 1st RSU and 2nd RSU are nearly identical, making it uncertain which RSU to select. As observed in Fig. 10, when the predicted values of the 1st and 2nd RSUs are close, the difference in simulated values is only around 3 dB. In such cases, it is more efficient to maintain the current RSU selection rather than switching between RSUs, as this minimizes unnecessary transitions while preserving communication quality.

The results of the bus and car running side-by-side are shown in Fig. 12. The red arrows highlight instances where the predicted values, which guided RSU selection, deviated from the actual simulation values. Specifically, between positions No. 6 and No. 10, spanning approximately 2 meters, the 2nd RSU was selected, even though the 1st RSU would have provided higher received power. One potential cause for this discrepancy is the limited accuracy of the predicted values. In this scenario, a large bus crosses the street alongside a smaller vehicle, and as indicated by the 1st RSU's simulated values (blue), the degree of shielding is influenced by the size of the vehicles. The observed error may stem from a mismatch between the simulated and predicted values—the simulated values exhibit a stair-stepped pattern, while the predicted values are smoother. This difference likely contributed to the incorrect RSU selection in this range.

The results of the bus and car running in opposite lanes are shown in Fig. 14. Unlike the scenarios in Figs. 8 and 10, the large body of the bus immediately obstructs the 2nd RSU from the start, leading to the consistent selection of the 1st RSU. In contrast to Fig. 12, no errors were observed in this scenario. This may be attributed to the relative simplicity of the setup, where the bus and car pass each other in opposite lanes, resulting in less complex shielding dynamics compared to the scenario where the vehicles run side-by-side.

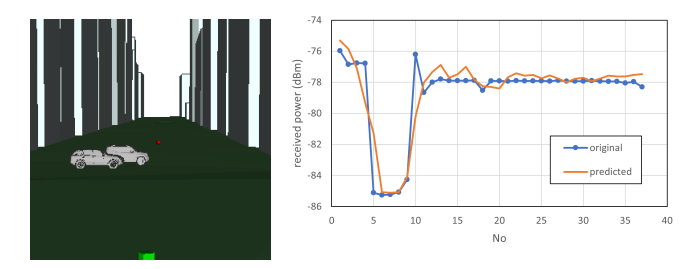


Fig. 7: Car and jeep running side-by-side (2nd RSU).

#### C. Discussion

As illustrated in Fig. 1, the distances between the receiver and the 1st RSU and 2nd RSU are 67 m and 56 m, respectively. Consequently, in a Line-of-Sight (LOS) environment, the 2nd RSU, being closer to the receiver, typically achieves a higher

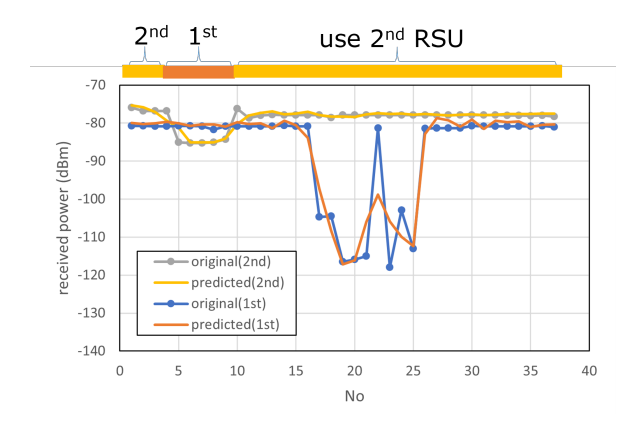


Fig. 8: Car and jeep running side-by-side (with RSU selection).

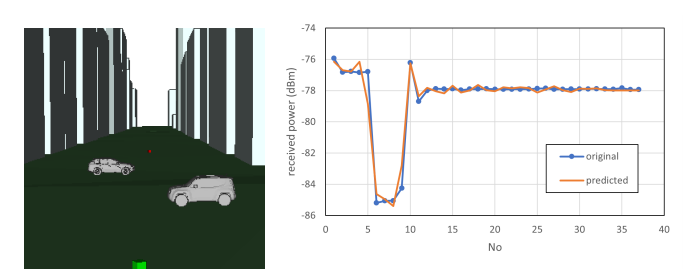


Fig. 9: Car and jeep running in opposite lane (2nd RSU).

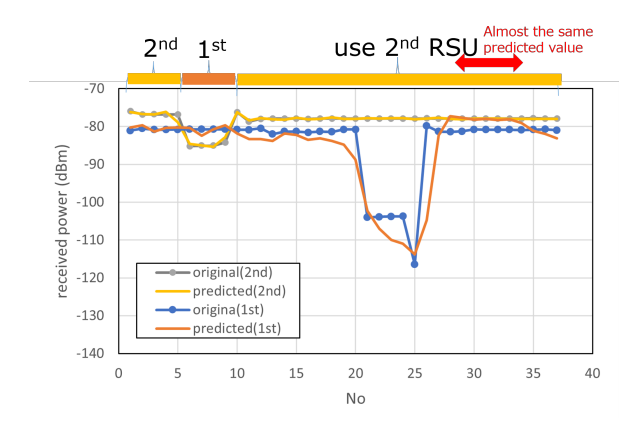


Fig. 10: Car and jeep running in opposite lane (with RSU selection).

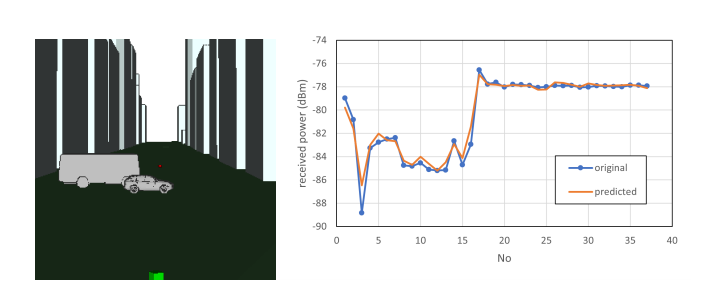


Fig. 11: Bus and car running side-by-side (2nd RSU).

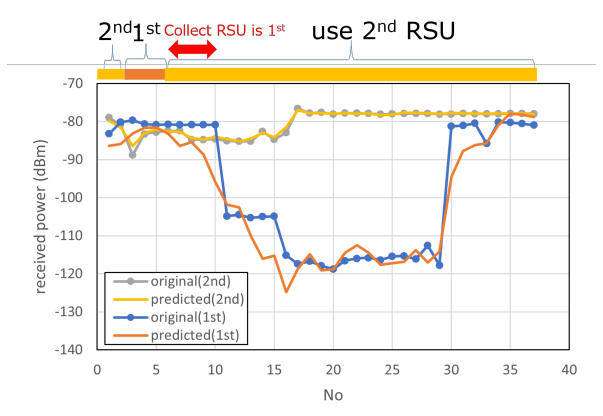


Fig. 12: Bus and car running side-by-side (with RSU selection).

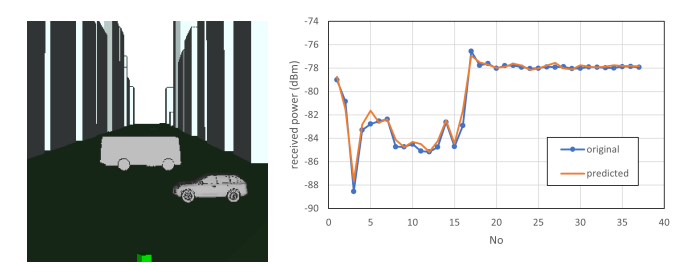


Fig. 13: Bus and car running in opposite lane (2nd RSU).

received power. However, when the 2nd RSU is obstructed, the 1st RSU, positioned directly in front of the receiver, often maintains LOS connectivity. We believe that optimal V2X communication can be achieved by leveraging these two RSUs dynamically, ensuring consistent and reliable performance regardless of shielding conditions.

Another factor contributing to the higher received power of the 2nd RSU may be reflections from nearby buildings. When the 1st RSU is positioned directly in front of the receiver, there are no reflective walls at the intersection, resulting in fewer reflection paths to the receiver. In contrast, the 2nd

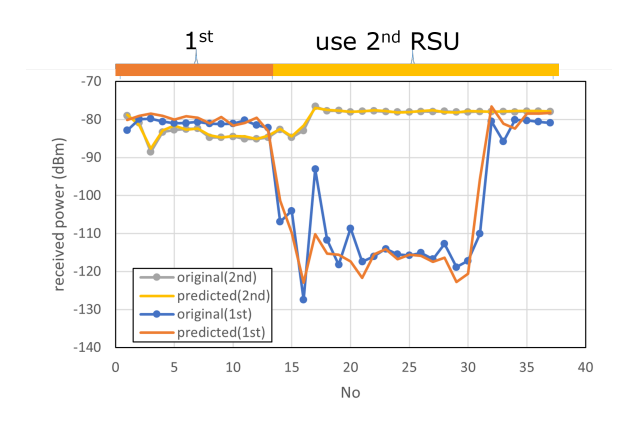


Fig. 14: Bus and car running in opposite lane (with RSU selection).

RSU, positioned diagonally to the left, benefits from additional reflection paths due to the building located alongside the road where the receiver is positioned. The reflection paths from both the 1st and 2nd RSUs are illustrated in Figs. 15 and 16. In the text, "D" represents diffraction paths associated with the 1st RSU, while "R" indicates reflection paths associated with the 2nd RSU.

Based on the discussion so far, we propose a system model for RSU selection, as illustrated in Fig. 17. In this model, cameras and antennas installed on the RSUs capture images and measure the received power of vehicles at the intersection. This data is then transmitted to a server for deep learning and computational processing. Once the system predicts the future received power, it dynamically controls and switches between RSUs to optimize communication.

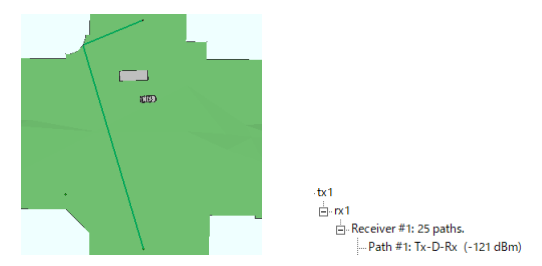


Fig. 15: Path from the 1st RSU.

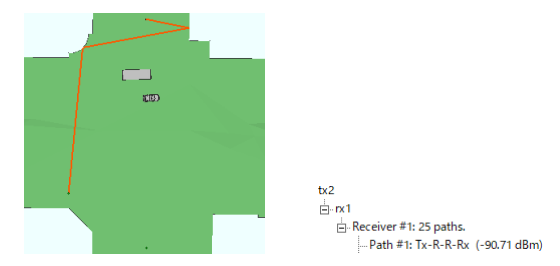


Fig. 16: Path from the 2nd RSU.

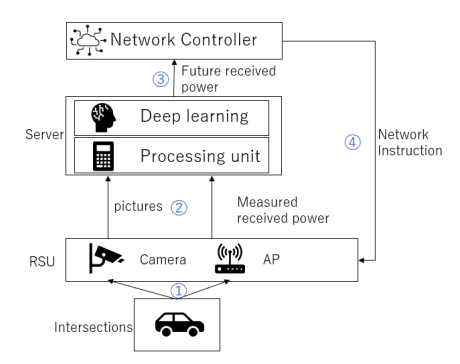


Fig. 17: Our proposed RSU selection mechanism.

## IV. CONCLUSION

This paper aims to predict V2I communication performance in dynamic traffic environments using camera images. For physical layer emulation, Wireless InSite was used to mimic the propagational mechanisms and shielding effects of mm-Wave V2I communications at large-scale intersection environments. In our simulation environments, 3D city models from Plateau was used, allowing vehicles to be positioned flexibly, significantly expanding the scope of the simulations. We modeled multiple vehicles and analyzed how received power varied in scenarios where vehicles were running side-by-side or passing each other. When the optimal RSU with the highest predicted received power was selected based on image-derived predictions, the error between the simulated and predicted values was minimal. These results demonstrate that the prediction-based RSU selection achieved sufficient accuracy for effective communication management.

In the future, we aim to expand the number of scenarios and perform simulations involving multiple RSUs. Enhancing the quality of the training data will be a key priority. Specifically, it will be important to identify the types of discrepancies between the simulation and real-world environments and evaluate the extent to which these discrepancies influence machine learning outcomes. Additionally, we plan to analyze how increasing the number of RSUs impacts overall communication quality and explore the potential improvements this approach can provide.

#### REFERENCES

- [1] A. Pundir, S. Singh, M. Kumar, A. Bafila and G. J. Saxena, "Cyber-Physical Systems Enabled Transport Networks in Smart Cities: Challenges and Enabling Technologies of the New Mobility Era," in IEEE Access, vol. 10, pp. 16350-16364, 2022.
- [2] Z. Li, T.Yu, R. Fukatsu, G. K. Tran, and K. Sakaguchi, "Towards Safe Automated Driving: Design of Software-Defined Dynamic MmWave V2X Networks and PoC Implementation," IEEE Open Journal of Vehicular Technology, pp. 1, Jan. 2021.
- [3] W. Tong, A. Hussain, W. X. Bo, and S. Maharjan, "Artificial Intelligence for Vehicle-to-Everything: A Survey," in IEEE Access, vol. 7, pp. 10823-10843, 2019.
- [4] M. Sasaki, T. Nakahira, N. Kuno, M. Inomata, W. Yamada, and T. Moriyama, "Path Loss Variation Prediction at 2-26 GHz Band using LSTM," IEICE Technical Report, AP2020-112, 2021.
- [5] M. Sasaki, N. Shibuya, K. Kawamura, N. Kuno, M. Inomata, W. Yamada, and T. Moriyama, "RNN Based Proactive Prediction of Received Power Using Environmental Information," IEICE Technical Report, AP2022-36, 2022.
- [6] K. Inoue, K. Imaizumi, K. Ichige, T. Nagao, and T. Hayashi, "Path Loss Estimation Using Spatial Data and Neural Networks," IEICE Transactions on Communications, Vol. J105–B, No. 11, pp. 872–879, 2022.
- [7] S. Ito, S. Mihara, T. Murakami, and H. Shinbo, "Feasibility Study on Blockage Prediction with Machine Learning in Outdoor mm-Wave Environmen," IEICE Technical Report RCS2020-59, p. 7-12, 2020.
- [8] S. Bannai and K. Suto, "Fast Blockage Prediction with Stereo Vision for mmWave V2X Communications," IEICE Technical Report SR2023-68, p. 99-101, 2023.
- [9] H. Okamoto, T. Nishio, M. Morikura, D. Murayama, and K. Nakahira, "Realtime Throughput Estimation Using Depth Images for mmWave Communications," IEICE Technical Report SR2016-55, p. 1-6, 2016.
- [10] Wireless Insite, Ver. 3.4.4, Remcom, USA, (2023).
- [11] Ministry of Land, Infrastructure, Transport and Tourism, "PLATEAU, " [Online]. Available: https://www.mlit.go.jp/plateau/. (accessed on 2024.12.27).